pH-Dependent Luminescence of Ruthenium(II) Polypyridine Complexes

Bingwen Jing, Tao Wu, Chunhong Tian, Manhua Zhang,*,# and Tao Shen

Center for Molecular Sciences, Chinese Academy of Sciences, Beijing 100080, P.R. China

(Received July 5, 1999)

The changes in the absorption and emission of three new complexes, $[Ru(bpy)_2L]^{2+}$(**1**—**3**), upon a pH variation are considered and the mechanism of the changes is discussed. The luminescence quantum yields of complexes **2** and **3** are strongly influenced by the pH due to intramolecular photoinduced electron transfer, which depends on the pH of the environment.

Recently, transition metal complexes (TMCs) with long-lived excited states have been widely used in solar energy conversion, biological probes and sensors.[1,2] Compared with the typical nanosecond organic probes, TMCs have many potential advantages as luminescence probes, including a long excited-state lifetime and a high luminescence quantum yield,[3] which make them much easier to detect and allow efficient time discrimination from the ubiquitous fluorescence of short-lived organic molecules. $[Ru^{II}L_3]^{2+}$ complexes (L = α-diimine) have been proven to be particularly versatile in these applications owing to their strong visible absorption, stability, efficient emissions, and long-lived excited states.[4,5] Furthermore, their emitting-state energies and excited redox properties can be extremely sensitive to variations in the coordination ligands and the local environment.[6—10] Many of these sensitizers exhibit a variety of energetically accessible charge transfers, ligand fields, and intraligand excited states that can have quite different characteristics. Understanding these allows the rational design of new, more useful sensitizers and probes. Ruthenium(II) polypyridine complexes as luminescence sensors have found many applications, for example, as oxygen sensors,[11,12] pH sensors,[13,14] carbon dioxide sensors,[15,16] specific metal ion sensors,[17] and temperature sensors.[18]

Changes in the absorption spectra for species having pH-dependent ground state chemistry can be used in quantitative pH determinations or as titration indicators. Absorption spectral changes are rather insensitive and difficult to use in remote fiber optics and small pH-based sensors. However, luminescent molecules that show pH-dependent changes in the luminescence spectra can be used as sensitive pH indicators. Generally, three strategies are adopted in designing a pH-sensor based on ruthenium complexes.[2] The first is introducing auxiliary ligands with one or more pH-sensitive groups, such as CN, 4,7-$(OH)_2$phen, into a ruthenium complex. The second is building a composite molecule having a luminescent moiety covalently attached to a fragment that is pH sensitive and can quench the excited portion differently depending on protonation. The third is indirect quenching, which depends on a very efficient dipole–dipole or Förster resonance energy transfer occurring between an excited and a ground state molecule. Although, to date, only a few pH sensors based ruthenium complexes have been reported,[13,14] we now report on the synthesis and photophysical properties of a few new ruthenium polypyridine complexes because their remarkably pH-dependent photophysical properties make them promising candidates of pH sensors.

Present Mailing Address: Institute of Photographic Chemistry, Chinese Academy of Sciences, Beijing 100101, P.R. China.

Experimental

Chemicals: 2,2′-Bipyridine (bpy), 1,10-phenanthroline (phen), and $RuCl_3 \cdot xH_2O$ (Aldrich) were commercial samples and used without purification; all other reagents were used as received from chemical supplies.

Syntheses: $[Ru(bpy)_2Cl_2] \cdot 2H_2O$[19] and 1,10-phenanthroline-5,6-dione(phendione)[20] were synthesized using the literature methods. The syntheses of **1**—**3** are summarized in Scheme 1.

General Preparation for Ligands: A mixture of 1 mmol 1,10-phenanthroline-5,6-dione, 1.4 mmol aldehyde, 8 ml glacial acetic acid, and 1.6 g ammonium acetate in a 50 ml flask with a condenser was refluxed for 1 h; after cooling, this mixture was diluted with water and neutralized with concd aqueous ammonia, immediately resulting in a yellow or light-yellow precipitate, which was washed with water, acetone, dichloromethane, and diethyl ether respectively, and then dried. The pure products were obtained by recrystallization or by column chromatography on silica gel.

L_1: 525 mg (2.5 mmol) 1,10-phenanthroline-5,6-dione, 0.4 ml (3.5 mmol) formaldehyde, 37 wt% solution in water, 20 g glacial acetic acid, and 4 g ammonium acetate gave 480 mg L_1, yield: 87 %. ^{1}H NMR (DMSO-d_6) δ = 9.06—9.06 (unresolved dd, 2H), 8.87—8.84 (unresolved d, 2H), 8.50 (s,1H), 7.87—7.83 (unresolved dd, 2H). Elemental Analysis, Calcd for $C_{13}H_8N_4$: C, 70.90; H, 3.66; N; 25.44%. Found: C, 70.25; H, 3.82; N: 26.01%.

L_2: 420 mg (2 mmol) 1,10-phenanthroline-5,6-dione, 418 mg (2.8 mmol) 4-dimethylaminobenzaldehyde, and 20 ml glacial acetic acid, and 3 g ammonium acetate gave L_2 529 mg, yield: 78%. ^{1}H NMR (DMSO-d_6) δ = 9.04—9.02 (m, 4H), 8.17—8.13 (dd, 2H), 7.91—7.89 (m, 2H), 6.90—6.88 (dd, 2H), 3.02 (s, 6H). Elemental Analysis, Calcd for $C_{21}H_{17}N_5$: C, 74.32; H, 5.05; N, 20.63%. Found: C, 74.78; H, 4.82; N, 21.12%.

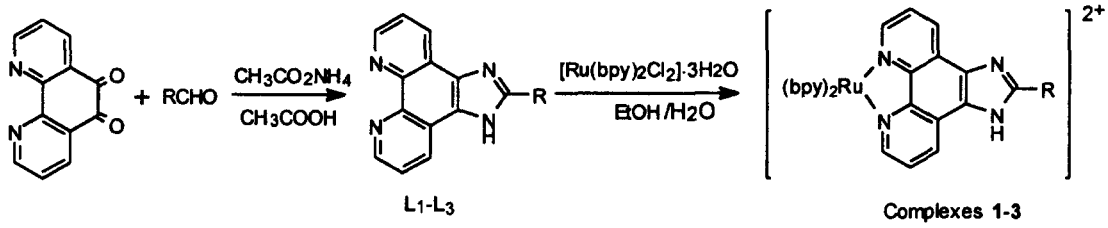

(1. R=-H, 2. R=-4-N,N-Dimethylphenyl, 3. R=-3-OMe-4-OH-Phenyl)

Scheme 1. The structures and the synthetic route of complexes **1**, **2**, **3**.

L_3: 525 mg (2.5 mmol) 1,10-phenanthroline-5,6-dione, 456 mg (3 mmol) 4-hydroxy-3-methoxybenzaldehyde, 20 ml glacial acetic acid, and 3.5 g ammonium acetate gave L_3 727 mg, yield: 85%. ^{1}H NMR (DMSO-d_6) δ = 9.54 (s, 1H), 9.04—9.02 (m, 2H), 8.95—8.92 (unresolved dd, 2H), 7.85—7.83 (unresolved dd, 2H), 7.80—7.70 (unresolved dd, 2H), 7.02 (d, 1H), 3.96 (s, 3H). Elemental Analysis, Calcd for $C_{20}H_{14}N_4O_2$: C, 70.17; H, 4.12; N, 16.37%. Found: C, 69.55; H, 3.98; N: 16.75%.

General Preparation for Ruthenium Complexes: A mixture of 0.2 mmol $[Ru(bpy)_2Cl_2]\cdot 2H_2O$, 0.2 mmol ligand, 20 ml ethanol–water (3 : 1, v/v) become deep yellow after refluxing under N_2 for 5 h; it was then cooled, and 10 ml saturated aqueous $NaClO_4$ was added. The resulting precipitate was separated by vacuum filtration, washed with chilled water and diethyl ether, and dried under vacuum. The crude product was purified by silica column chromatography using 2 : 1 (v/v) acetone/toluene as an eluant. The eluant containing the desired product was evaporated under reduced pressure and the product was obtained by recrystallization in acetone/toluene (1 : 1, v/v).

1. ^{1}H NMR (acetonitrile-d_3) δ = 8.98—8.95 (dd, 2H), 8.57—8.50 (q, 4H), 8.41 (s, 1H), 8.07 (ddd, 2H), 7.99—7.96 (m, 4H), 7.84—7.82 (dd, 2H), 7.74—7.72 (q, 2H), 7.55—7.54 (m, 2H), 7.42 (m, 2H), 7.18 (m, 2H). Elemental Analysis, Calcd for $Ru(C_{33}H_{24}N_8)\cdot 2ClO_4\cdot 3H_2O$: C, 44.71; H, 3.41; N, 12.64. Found: C, 45.01; H, 3.52; N, 12.93%. Yield, 75%.

2. ^{1}H NMR (acetonitrile-d_3) δ = 8.88 (dd, 2H), 8.57—8.51 (t, 4H), 8.07 (t, 2H), 7.94—7.83 (m, 8H), 7.64—7.59 (m, 4H), 7.43 (t, 2H), 7.23 (t, 2H), 6.70—6.67 (d, 2H), 2.96 (s, 6H). Elemental Analysis, Calcd for $Ru(C_{41}H_{33}N_9)\cdot 2ClO_4\cdot 2H_2O$: C, 49.86; H, 3.78; N, 12.76%. Found: C, 50.02; H, 3.85; N, 12.53%. Yield, 58%.

3. ^{1}H NMR (acetonitrile-d_3) δ = 8.90—8.88 (d, 2H), 8.57—8.50 (t, 4H), 8.08—8.07 (td, 2H), 7.97—7.74 (m, 8H), 7.65—7.60 (m. 4H), 7.46—7.42 (td, 2H), 7.25—7.23 (t, 2H), 6.83 (d, 1H), 3.85 (s, 3H). Elemental Analysis, Calcd for $Ru(C_{40}H_{30}N_8O_2)\cdot 2ClO_4\cdot 3H_2O$: C, 47.72; H, 3.60; N, 11.13%. Found: C, 47.61; H, 3.72; N, 10.91%. Yield, 73%.

Spectrometric Measurements: ^{1}H NMR spectra data were recorded in DMSO-d_6 or acetonitrile-d_3 with a Varian 300 MHz spectrometer. Absorption measurements were made with a Shimadzu UV-160A UV-visible spectrophotometer, emission spectra were recorded on a Hitachi 850 fluorescence spectrometer, and are reported uncorrected. Time-resolved luminescence measurements were performed with a time-domain fluorescence spectrometer (Horiba NAES-1100 model). The quantum yields were obtained using $[Ru(bpy)_3]^{2+}$ in water as an actinometer. Elemental analyses were carried out using a Heraeus CHN-Raid. Triply distilled water was used to prepare phosphate buffers, with pH values determined precisely using a pH-meter. Absorption and emission titrations were made in phosphate buffers. All spectrophotometric measurements were carried out under aerated solutions and at room temperature. unless otherwise stated.

Results and Discussion

Absorption and Emission. The photophysical data of the complexes are listed in Table 1. Compounds **1**, **3** exhibit strong room-temperature emission both in acetonitrile and in neutral water, but only **2** shows very weak room-temperature emission under the same conditions, which results from intramolecular electron transfer from *N*,*N*-dimethylaniline (DMA) to the MLCT excited state of the complex. This was verified through the emission quenching of complex **1** by DMA in acetonitrile.

The photophysical and electrochemical data are listed in Table 2.

The much higher energy of excited state of DMA makes energy transfer impossible from the excited complex **1** to DMA. According to the Rehm–Weller equation.[21]

$$\Delta G = E_{Ox}(D) - E_{Red}(A) - E_{0-0} - C \quad (1)$$

where $E_{Ox}(D)$ represents the oxidation potential of the donor, $E_{Red}(A)$ is the reduction potential of the acceptor, E_{0-0} is the singlet state energy of the sensitizer, and C is the stabilizing energy of $D^{+\cdot}A^{-\cdot}$, which can usually be regarded as 0.06 eV in a polar solvent.[22] The free-energy variation of the electron-

Table 1. Photophysical Data of Complexes **1**, **2**, and **3**

Complex	λ (MLCT)	τ (ns) in CH_3CN		λ_{em}^{max}		in CH_3CN		In water	
	($10^{-4}\varepsilon$)	Aerated	Degassed	In CH_3CN	In water	$10^3\,\phi'$	$10^3\,\phi$	$10^3\,\phi'$	$10^3\,\phi$
1	453.5 (1.661)	150	762	623	624	16.16	2.83	12.95	7.44
2	457.5 (2.40)	—	—	625	614	1.52	0.01	1.21	0.74
3	459.5 (2.18)	157	979	617	618	12.34	1.64	11.52	7.75

ϕ' and ϕ are the quantum yields under degassed and aerated conditions respectively, which are reported in comparison with an aerated solution of $[Ru(bpy)_3]\cdot[PF_6]_2$ in acetonitrile (ϕ = 0.012) from *J. Am. Chem. Soc.*, **104**, 6620 (1982). Excitation wavelength is 450 nm.

Table 2. The Photophysical and Electrochemical Data of Complex **1**, DMA[a)]

	E_{Ox} (eV)	E_{Red} (eV)	E_s (eV)	E_T (eV)
1	1.32[a)]	−1.28[a)]		2.30[b)]
DMA	0.81		3.85	2.99

E_{Ox} (eV)-oxidation potential, E_{red} (eV)-reduction potential, E_s (eV)-singlet energy, E_T (eV)-triplet energy. a) Redox potentials are reported vs. SCE in acetonitrile unless otherwise noted and are cited from Ref. 12. b) Measured with an M270 electrochemical system at a sweep rate of 100 mV s^{-1} in CH_3CN containing 0.1 M *n*-butylammonium perchlorate (1 M = 1 mol dm^{-3}) and with a Pt disc-working electrode and a Pt wire counterelectrode. c) Obtained from the intersection of the lowest energy absorption with the emission band.

transfer process from DMA to excited complex **1** is

$$\Delta G = E_{Ox}(\text{DMA}) - E_{Red}(\mathbf{1}) - E_{0\text{-}0}(\mathbf{1}) - C$$
$$= 0.81 - (-1.28) - 2.30 - 0.06 = -0.27 < 0 \quad (2)$$

Thus, an electron transfer from DMA to excited-state complex **1** is feasible. The bimolecular quenching constant, k_q^s, of 2.16×10^8 s^{-1} L mol^{-1} was obtained from a plot of ϕ_0'/ϕ' vs. [DMA] in acetonitrle accordance to Stern–Volmer equation,[23] where ϕ_0' and ϕ' are the emission quantum yields in the absence and the presence of DMA, respectively. At the same time, the excited-state lifetime quenching of **1** by DMA was measured in the same serial solution, and gave a lifetime quenching constant, k_q^D, of 2.12×10^8 s^{-1} L mol^{-1}, which is in agreement with k_q^s obtained from a steady measurement. This indicates that the quenching described above is a dynamic mechanism, and that no interaction in the ground state exists between complex **1** and DMA.

Both in acetonitrile and in water solution, the quantum yields under degassed conditions are larger than those under aerated conditions, which suggests that oxygen can efficiently quench the emission of these complexes. However, in two different solutions, the effect of oxygen on the emission of the complex is not the same. We observed a lower emission quantum yield in degassed water than that in degassed acetonitrile, while under an aerated condition, the emission quantum yield in water was higher than that in acetonitrile. The former may have resulted from a large non-radiative deactivation caused by the O–H vibration of H_2O around the ligand in water[24] and the hydrogen bonding interaction between the C–H bond in bpy and water. The latter is due to the different oxygen solubilities in the two solutions, because the solubility of oxygen at room temperature in acetonitrile is much larger than that in water. Similarly, the lifetimes of these complexes in aerated acetonitrile are much shorter than those in degassed acetonitrile.

Effect of pH on Absorption and Emission. Absorption Titration. The lowest excited state of polypyridine ruthenium complexes, for example, $[Ru(bpy)_3]^{2+}$, is assigned to the triplet excited state of a metal-to-ligand charge transfer (MLCT). The close similarity in the electronic absorption and emission spectra of $[Ru(bpy)_3]^{2+}$ and complexes **1**, **2**, **3** suggests the MLCT assignment for the lowest excited states in the latter complexes.

Below pH 3, the metal-to-ligand charge-transfer (MLCT) bands of complexes **1**—**3** are broad compared to those in neutral water or in acetonitrile (Fig. 1a as an example). With increasing pH, the shapes of the MLCT bands gradually restore to that in neutral water. Meanwhile, their absorption maximum shifts slightly to the red along with a slight increase in the intensity. In addition, the ultraviolet absorption in the range 300—400 nm for complexes **1** and **3** has very little pH-dependence. However, the ultraviolet absorption for complex **2** in the same range exhibits the obvious changes shown in Fig. 1a. Going from pH 3 to pH 12, the MLCTs bands of the three complexes show little change in shape, except from a little bathochromic shift on the absorption onset; also, their absorption intensities gradually and slightly increase for **1**, but decrease for **2** and **3** (such an example is shown in Fig. 1b).

Above pH 3, these complexes show significant variations of the absorption spectra in the ultraviolet region, especially for **2** and **3** (Fig. 1b). Distinct isosbestic points of 376 nm for **1**, 364 nm, 471 nm for **2**, and 472 nm for **3** were observed. From plots of the absorbance vs. pH (Fig. 2), the ground state pK_a values of compounds **1**—**3** were estimated, and are listed in Table 3.

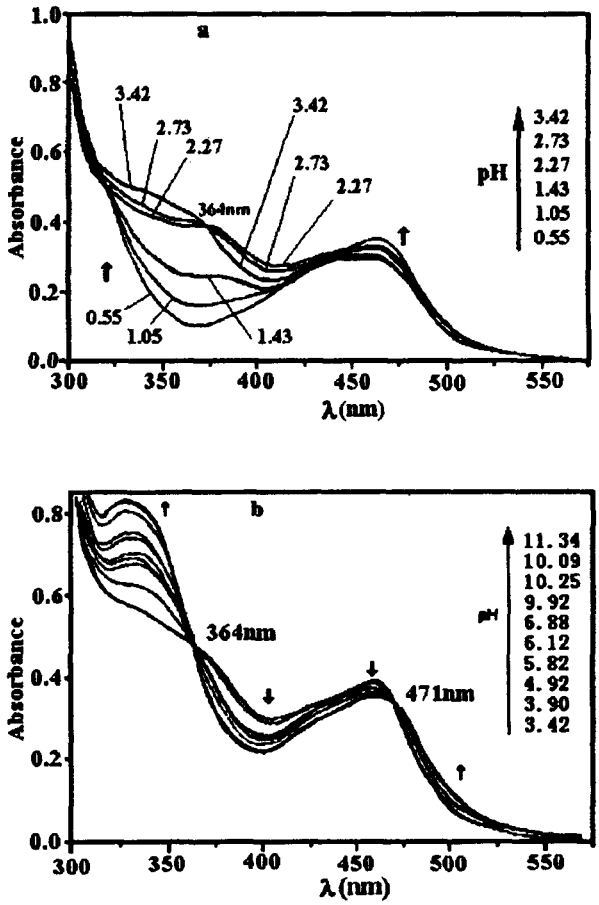

Fig. 1. Absorption spectral variations of **2** as a function of pH in phosphate buffers. a. pH 0.55—3.42, b. pH 3.42—11.34.

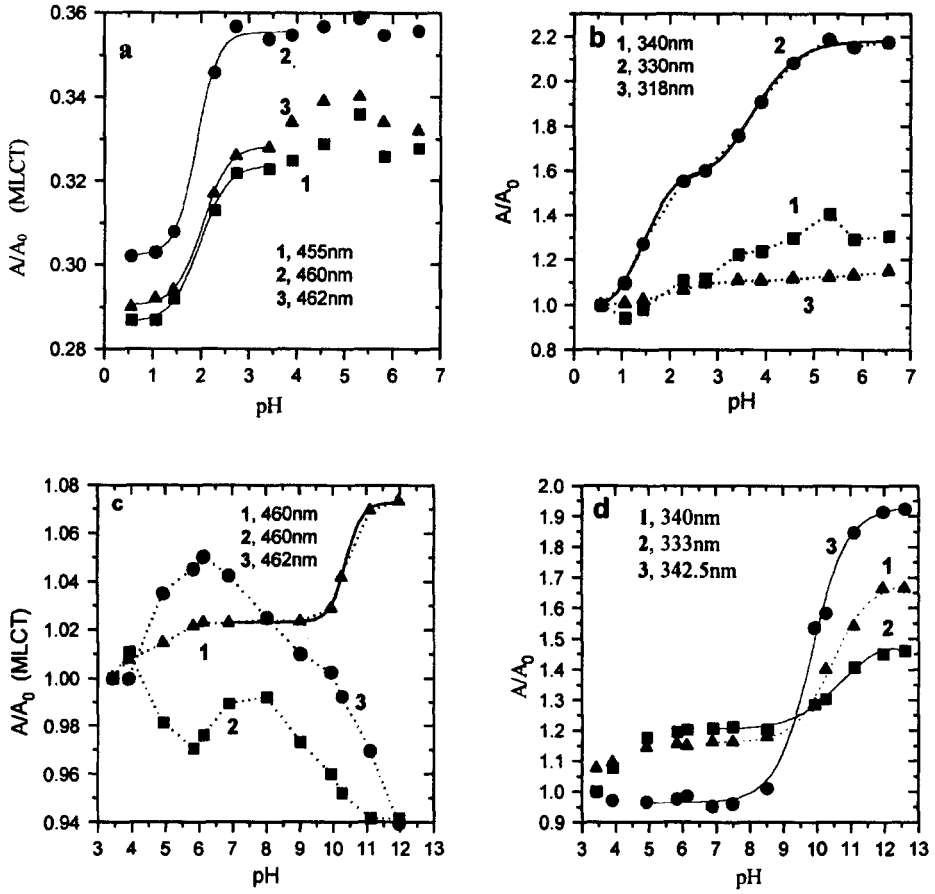

Fig. 2. The variation of absorbances with pH at given wavelength. (a) pH 0.55—7, MLCT absorption, at 455, 460, 462 nm for **1**, **2**, **3**, respectively. (b) pH 0.55—7, at 340, 330, 318 nm for **1**, **2**, **3**, respectively. (c) pH 3—13 MLCT absorption at 460, 460, 462 nm for **1**, **2**, **3**, respectively. (d) pH 3—13, at 340, 333, 342.5 nm for **1**, **2**, and **3**, respectively. *A* equals the value of absorbance of complexes **1**—**3** at different pH; A_0 equals the value of absorbance of complexes **1**, **2**, **3** at the indicated wavelength at pH 0.55 in Figs. a and b, and the values of absorbance for complex **1** at pH 2.73 and for complexes **2**, **3** at pH 3.42 in Figs. c and d.

Table 3. The pK_a Values of Complexes **1**, **2**, and **3**[a)]

Complex	pK_{a1} (abs.)	pK_{a2} (abs.)	pK_{a3} (abs.)	pK_{a1} (lum.)	pK_{a2} (lum.)	pK_{a3} (lum.)
1	1.97[b)]	10.48,[b)] 10.46[c)]		2.88	10.66	
2	1.97[b)]	3.75[c)]	10.56[c)]		4.22	10.71
3	1.97[b)]	9.50[c)]			6.71	

a) Solutions were made up in phosphate buffers. pH range 0.55—12.6. b) From MLCT. c) From ultraviolet region absorption variation. pK_a(abs.) and pK_a(lum.) were calculated using the Henderson–Hasselbalch-type mass action equations: (1) $\log[(A_{max}-A)/(A-A_{min})] = pK_a(abs.)-pH$, and $\log[(\phi_{max}-\phi)/(\phi-\phi_{min})] = pK_a(lum.)-pH$, respectively.

Emission Titration. As with $[Ru(bpy)_3]^{2+}$, the emissions of compounds **1**, **2**, **3** come from the metal-to-ligand change transfer (MLCT) excited states, which are sensitive to their environments. From pH 0.55 to pH 13, the shapes of the emission spectra of **1**—**3** are preserved. The emission maxima exhibit an obvious blue shift with increasing pH from 0.55 to 11, and in a high pH range larger than 11 they show a slight red shift (Fig. 3). From pH 0.55 to pH 7, the emission spectra exhibit a ca. 17, 16, 12 nm blue shift for **1**, **2**, and **3** respectively. The luminescence quantum yield (ϕ) –pH profiles of complexes **2**, **3** are sigmoidal with a negative gradient, which is due to photoinduced intramolecular electron transfer from the side-chain group to the MLCT excited state of the complex (Fig. 4). Compared with **1**, the greater degree of luminescence quenching is for **2**, and the greatest degree of luminescence quenching is for **3**. In addition, the ϕ–pH profiles show two inflection points for **2** and one for **3**, respectively, in the range of pH 0.55—11 (Table 4). In contrast with **2**, **3**, the ϕ–pH profile of complex **1** is bimodal, comprising two sigmoidal curves of opposite gradients. When the pH is low (pH = 0.55) enough to protonate the *tert* N on the imidazole ring, the location of the positive charge in the vicinity of ruthenium(II) may quench the emission of complex,[14] which results in lower lumines-

Table 4. Photophysical Data of Complexes **1**, **2**, **3** at Selected pH Value[a)]

Complex	1			2			3		
pH	λ_{em}^{max}	λ_{abs}^{max}	$\phi \times 10^3$	λ_{em}^{max}	λ_{abs}^{max}	$\phi \times 10^3$	λ_{em}^{max}	λ_{abs}^{max}	$\phi \times 10^3$
1	638	435	34.9	644	436	44.6	635	436	46.0
3	634	453	39.6	634	458	33.3	632	458	46.5
7	622	455	41.6	628	460	9.0	620	460	12.5
12	632	458	26.4	632	462	3.69	630	461	0.51

a) Quantum yields were measured in aerated solution by comparison with $[Ru(bpy)_3]^{2+}$ in aerated water (M. J. Cook, A. P. Lewis, et al., *J. Chem. Soc., Perkin Trans. 2*, **1984**, 1293). All values reported are measured in phosphate buffers. Excitation wavelength is 450 nm.

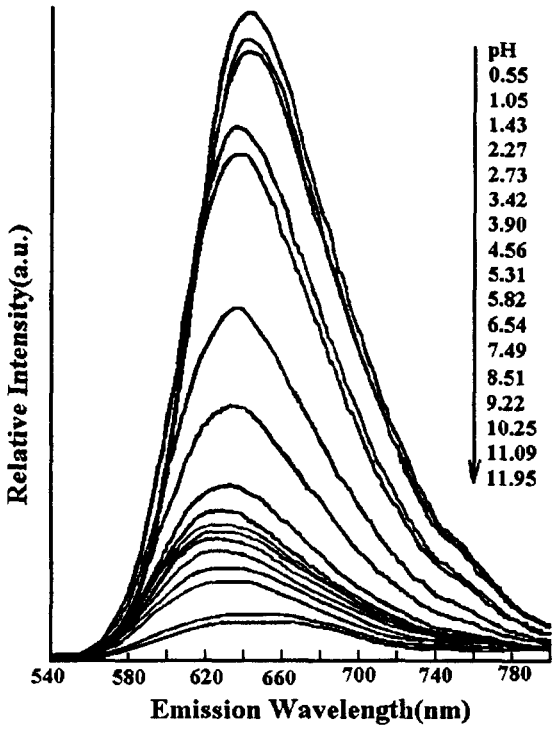

Fig. 3. Emission spectral variations of **2** as a function of pH in phosphate buffers. Excitation wavelength is 450 nm.

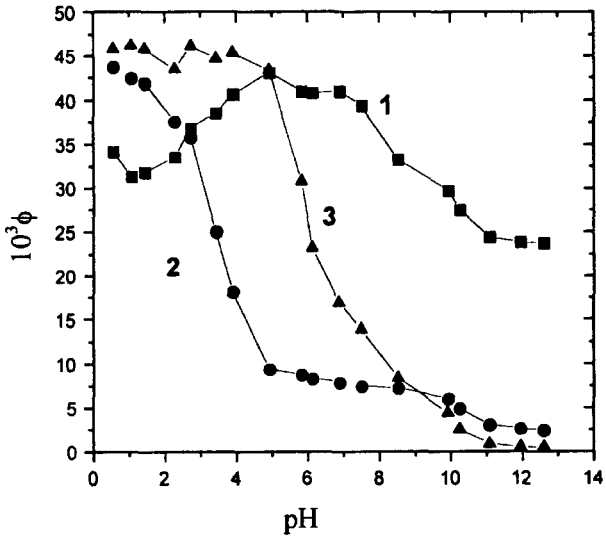

Fig. 4. Luminescence quantum yield (ϕ) for complexes **1**—**3** vs. pH in phosphate buffers. Quantum yields were measured on aerated solutions by comparison with $[Ru(bpy)_3^{2+}]$ in aerated water.[11] Excitation wavelength is 450 nm.

cence quantum yields being observed in the pH region from 1 to 5. Because deprotonation of *tert* N on the imidazole ring eliminates the positive charge, the retrieval of the quenched emission takes place, resulting in a segment of the ϕ-profile with a positive gradient.

When pH > 7, all of the nitrogen atoms on imidaziole are completely deprotonated, and the location of negative charge in the vicinity of ruthenium(II) (Scheme 2) may quench the luminescence by charge transfer to the MLCT excited state of the complex. The ϕ–pH profiles show a segment with a negative gradient from pH 7—13.

Since imidazole is a weak acid as well as a weak base. the acid-base properties of the medium will affect the absorption and emission of these complexes. With a pH variation, the predominant emitting species of **1** is the protonated from (I) (pH < 1), the neutral form (II) (pH 3—8), and the deprotonated from (III) (above pH 12), (Scheme 2). The pK_{al}(abs.) = 1.97 is smaller than pK_{al}(lum.) = 2.88 indicating that complex **1** in the excited state is a stronger base than in the ground state at a low pH. Similarly, we can obtain the pK_{a2} = 10.46, the pK_{a2}(lum.) = 10.66 from titration curves. Imidazole is a weak base, having a pK_{al} of 6.95, and the addition of a phenyl group to imidazole reduces the overall basicity. Further, the coordination with ruthemium(II) reduces the electron density of imidazole. Thus complex **1** shows a much weaker basicity than that of imidazole itself.

With the pH less than 1, the emission of **2** comes from form I (Scheme 3). With increasing pH, the *tert* N on the imidazole ring is deprotonated (pK_{al}(abs.) = 1.97), and thus the N of the *N*,*N*-dimethylanilino group is deprotonated along with a further pH increase, having a pK_{a2}(abs.) of 3.7, which is smaller than that of free DMA (pK_a = 4.4). This may be because the link of DMA with imidazole disperses the electron density on the N of DMA group, and reduces the overall basicity. Compared with **1**, the emission from **2** is much weaker in the range of pH 3—7, which is caused by an intramolecular electron transfer from DMA to the central excited-state ruthenium complex. It is well known that DMA is a strong electron donor, which can cause efficient photoinduced electron transfer with ruthenium(II) complexes

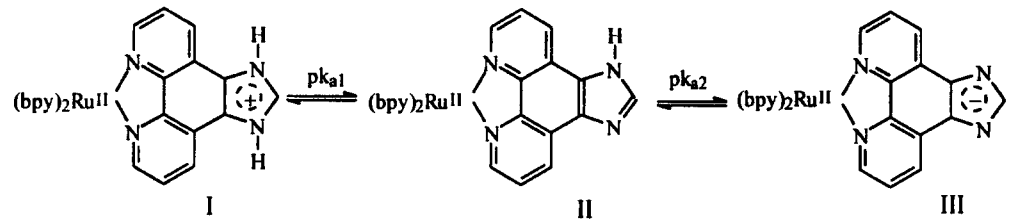

Scheme 2.

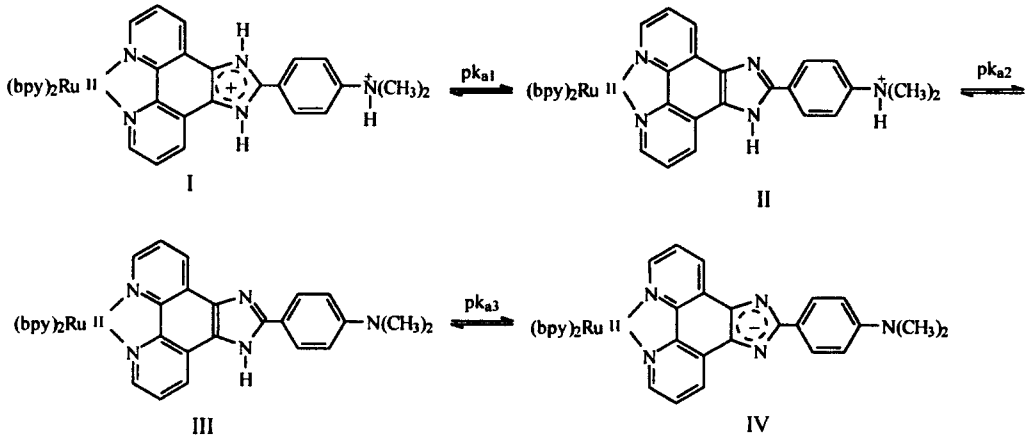

Scheme 3.

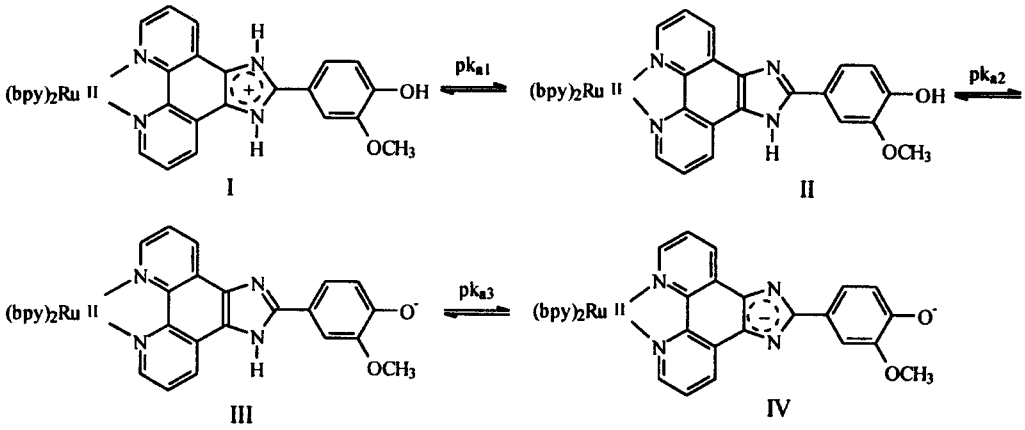

Scheme 4.

(Table 4).[14] Between pH 7—13, the emission of **2** was further quenched and another inflection was observed with a pK_a(lum.) of 10.71, consistent with the second dissociation constant of imidazole. At the pH > 12, the luminescence of **2** mainly comes from form IV (Scheme 3), and the luminescence is the result of electron-transfer quenching.

There is also the acid-base equilibrium for **3** (Scheme 4). From its absorption titration curves vs. pH, two pK_a(abs.)s of 1.97 and 9.50 are obtained, with the former corresponding to the first dissociation constant of imidazole and the latter consistent with O-methoxyphenol's ionization constant. With increasing pH, the luminescence of complex **3** is sharply quenched with a pK_a of 6.71, which is smaller than that obtained from absorption titration, demonstrating that phenole in the excited-state of **3** is a stronger acid than in the ground-state. The phenoxide anion formed in basic solution is a strong electron donor. The electron-transfer reactions between phenols and ruthenium(II) polypyridine complexes have already been reported[13,25] and have been used in the determination of the ionization equilibrium constants of phenols.[26] The formation of the phenoxide anion causes a photoinduced intramolecular electron transfer from the phenoxide ion to the polypyridine ruthenium(II) moiety.

Conclusion

The luminescence pH-sensitivity of ruthenium(II) polypyridine complexes has been achieved through intramolecular electron-transfer quenching by the DMA or phenol moiety, which are, themselves, pH sensitive. Luminescence titration shows that the emission yields of complexes **2** and **3** vary considerably with the pH, which is the basis of the ruthenium complex used as pH–luminescence sensors. Therefore, complexes **2**—**3** are promising candidates for luminescent pH sensors.

This research was supported by the National Natural Science Foundation of China (No: 59783007).

References

1 Y. Shen and B. P. Sullivan, *J. Chem. Educ.*, **74**, 685 (1997).
2 J. N. Demas and B. A. DeGraff, *J. Chem. Educ.*, **74**, 689 (1997).
3 J. N. Demas and B. A. DeGraff, *Anal. Chem.*, **63**, 829A (1991).
4 K. Kalyanasundaram, *Coord. Chem. Rev.*, **46**, 159 (1982).
5 R. J. Watts, *J. Chem. Educ.*, **60**, 834 (1983).
6 P. C. Ford, *Rev. Chem. Intermed.*, **2**, 267 (1979).
7 C. Creutz, M. Chou, T. L. Netzel, M. Okumura, and N. Sutin, *J. Am. Chem. Soc.*, **102**, 1309 (1980).
8 G. A. Reitz, J. N. Demas, E. Stephens, and B. A. DeGraff, *J. Am. Chem. Soc.*, **110**, 5051 (1988).
9 L. Sacdstedr, J. N. Demas, and B. A. DeGraff, *Inorg. Chem.*, **28**, 1787 (1989).
10 E. Kraus and F. Ferguson, *Prog. Inorg. Chem.*, **37**, 293 (1989).
11 J. R. Bacon and J. N. Demas, *Anal. Chem.*, **59**, 278 (1987).
12 E. R. Carraway, J. N. Demas, B. A. Degraff, and J. R. Bacon, *Anal. Chem.*, **63**, 337 (1991).
13 R. Grigg, J. M. Holmes, S. K. Jones, and E. D. J. A. Norgert, *J. Chem. Soc., Chem. Commun.*, **1994**, 185.
14 R. Grigg and E. D. J. A. Norgert, *J. Chem. Soc., Chem. Commun.*, **1992**, 1300.
15 O. S. Wolfbeis, in "Molrcular Luminescence Spectroscopy Methods and Applications," ed by S. G. Schulman, Wiley, New York (1988), Part 2, p. 283.
16 A. Mills, Q. Ching, and N. McMurray, *Anal. Chem.*, **64**, 1383 (1992).
17 B. P. Sullivan, *J. Chem. Educ.*, **74**, 685 (1997).
18 J. N. Demas and B. A. DeGraff, *SPIE*, **1796**, 71 (1992).
19 B. P. Sullivan, D. J. Salmon, and T. J. Meyer, *Inorg. Chem.*, **17**, 3334 (1978).
20 C. Hiort, P. Licoln, and B. Norden, *J. Am. Chem. Soc.*, **115**, 3448 (1993).
21 G. J. Kararnos and N. J. Turro, *Chem. Rev.*, **86**, 401 (1986).
22 L. R. Faulkner, H. Tachikawa, and A. J. Bard, *J. Am. Chem. Soc.*, **94**, 691 (1972).
23 N. J. Turro, "Modern Molecular Photochemistry," Benjamin/Cummings, Menlo Park, CA (1978), p. 247.
24 J. Van Houten and R. J. Watls, *J. Am. Chem. Soc.*, **98**, 4853 (1976).
25 K. Miedlar and P. K. Das, *J. Am. Chem. Soc.*, **104**, 7462 (1982).
26 H. E. Gsponer, G. A. Arguello, and G. A. Arguello, *J. Chem. Educ.*, **74**, 968 (1997).